Thermodynamic Deformation of Wet Snow

by

S.C. Colbeck
U.S. Army Cold Regions Research
and Engineering Laboratory

Abstract

The deformation of wet snow is explained in terms of the thermodynamics of the three phases of water. When deformation by more efficient particle packings are no longer possible, deformation can occur most rapidly by melting at the particle contacts. The rate of deformation is highly sensitive to the liquid water content, ionic impurity content, particle contact area and stress level. A model of the hydrostatic deformation of wet snow is constructed and examples of the deformation of wet snow are given for a variety of conditions. These results compare favorably with existing experimental evidence. These results compare favorably with existing experimental evidence. The model accurately simulates the transient nature of the deformation and the effect of water content on the quasi-stable density of wet snow subjected to a constant stress.

List of Symbols

d	thickness of water film
D	height of melted cap
F	force between particles
k	thermal conductivity of ice
L	latent heat of fusion
n_s	moles of solute
n_w	moles of water
P_b	pressure at the bond
P_c	capillary pressure
q	water flux in film
Q	heat flux
r	polar coordinate
r_a	radius of air bubble
r_b	radius of inter-particle bond
r_o	initial particle radius
r_p	particle radius
R	gas constant for water vapor
T_b	temperature of bond
T_o	273 °K

T_s	temperature of curved particle surface
μ	viscosity of water
ρ	ice density of snow sample
ρ_ℓ	liquid water density
ρ_o	density of ice
$\sigma_{\ell g}$	liquid-vapor interfacial tension
$\sigma_{s\ell}$	solid-liquid interfacial tension

Introduction

The rheology of snow at subfreezing temperatures has been extensively researched and much useful information has been generated (see Mellor, 1975). Unfortunately the rheology of snow which contains liquid water has been almost totally ignored. This disparity does not arise because wet snow is any less important than snow at lower temperatures - witness the destructive powers of wet snow slides and highway hazards caused by the compaction of wet snow into ice - but probably arises because of the greater difficulty of handling samples of wet snow and of understanding the complex interaction between the thermodynamic and mechanical aspects of wet snow deformation.

For a given stress, the deformation of wet snow generally occurs much more rapidly than can be explained by intracrystalline straining and/or more efficient grain packing; hence, some thermodynamic explanation must be invoked. Colbeck (1973) described some of the important aspects of the phase thermodynamics of wet snow. The equilibrium temperature among the three phases of water in wet snow is controlled by the grain size, water content, grain-contact area, impurity content, porosity, and stress. These principles are used here to describe the thermodynamic deformation of wet snow at large strain rates. The slow deformation of wet snow in situations where intracrystalline creep or grain repacking are the dominate mechanisms is not considered but the limitations of this theory can be clearly delineated from the theory itself.

Thermodynamics

The thermodynamic deformation of wet snow is controlled by temperature differences among the inter-particle contacts and the ice-pore fluid interfaces (see Figure 1). The temperature at a contact is determined exclusively by the contact area and the average normal force acting across the contact. During rapid deformation no shear forces can be supported by a contact because the ice surfaces are separated by a water film of sufficient thickness to prevent ice-to-ice contact. The thickness of this film as determined by the rate of deformation is described later.

The temperature of the free surface away from the inter-particle contacts is determined by the radius of the particles, radius of the air-liquid interface and impurity content of the liquid phase in the pores. There are three possible temperature regimes:

1) When the surface temperature (T_s) is less than the contact temperature (T_b), heat flows away from the contact thus

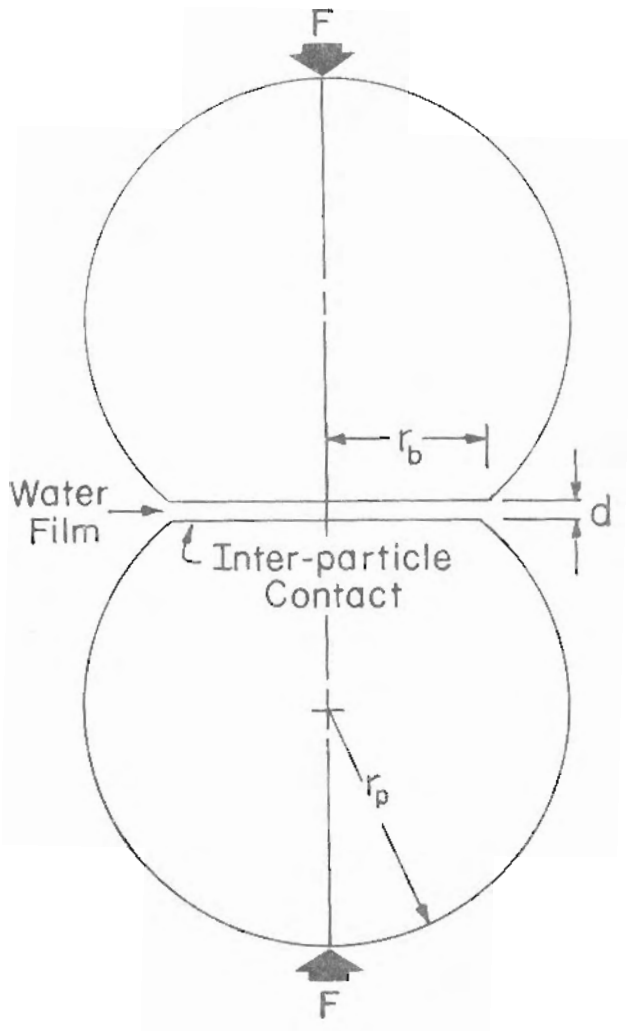

Figure 1.

Two particles move closer by melting at their mutual contact. Heat flow from the particle-pore fluid interface to the inter-particle contact causes melting at the contact. Melt water moves through the water film into the pore space and refreezes on the particle surface.

freezing the liquid layer, and causing a rapid development of inter-particle strength. This regime occurs when the snow is frozen by either spreading salt on a wet snow surface or by rapidly withdrawing the liquid. Then the relatively rapid thermodynamic deformation ceases and the wet snow deforms by the same mechanisms as cold snow. If a higher stress or more liquid are introduced, the contacts may melt again.

2) When the pore surface and contact temperatures are equal no heat flow occurs but a significant inter-particle strength can develop slowly as ice-to-ice adhesion develops. The liquid tension may cause some additional inter-particle forces (Moore and Millar, 1971; Skelton, 1975).

3) When the lowest temperature occurs at the inter-particle contact because of the depression of the phase equilibrium temperature by the contact stress, heat flows toward the contact causing a continuous melting of ice at the contact. This melting at the high pressure contact causes water to flow out of the contact toward the low pressure, pore water. Thus regelation is established whereby water flow and heat flow are balanced resulting in melting at the contact, refreezing on the free surfaces, and densification as the particle contacts move closer together and the pore space is reduced by refreezing.

This densification can be driven rapidly even at moderate stress levels by the forces transmitted across the contacts. The contact temperature during rapid densification is independent of impurities in the pore water because meltwater moves away from the contact. Accordingly, the equilibrium temperature (T_b) for the nearly flat contact surface, where the dissolved air is neglected because of uncertainty about the air content of the melt, is given by

$$T_b = \frac{P_b T_o}{L} \left(\frac{1}{\rho_\ell} - \frac{1}{\rho_s}\right) \qquad (1)$$

The phase-equilibrium temperature on the rounded particle surface depends upon the saturation regime of the wet snow (Colbeck, 1973). The equilibrium temperature in the funicular regime of high liquid saturation is determined by the ice particle (r_b) and air bubble (r_a) sizes according to,

$$T_s = \frac{2T_o}{L} \left(\frac{1}{\rho_\ell} - \frac{1}{\rho_s}\right) \frac{\sigma_{\ell g}}{r_a} - \frac{2T_o}{L\rho_s} \frac{\sigma_{s\ell}}{r_p} - \frac{RT_o^2}{L} \frac{n_s}{n_w} \qquad (2)$$

where the last term describes the temperature depression caused by the presences of ionic impurities. Similarly, the equilibrium in the pendular regime of low saturations is determined by the particle size, capillary pressure (P_c), and ionic impurities according to

$$T_s = -\frac{T_o}{\rho_\ell L} P_c - \frac{2T_o}{L\rho_s} \frac{\sigma_{sg}}{r_p} - \frac{RT_o^2}{L} \frac{n_s}{n_w} \qquad (3)$$

Ionic impurities, capillary pressure or small particle sizes reduce the temperature of the particles at the pore surfaces. The heat flow to the bonds is reduced accordingly. The rate of deformation, the ultimate bond size, and maximum density achievable by rapid thermodynamic densification are also reduced. In unstressed, saturated snow, particle size increases rapidly to the quasi-stable diameter of 1 to 3 mm (Wakahama, 1968; Colbeck, 1973). At that time the effect of particle size on the phase equilibrium temperature is only 10^{-4} to 10^{-5} °C, or about the same as the effect of impurities in natural snow.

Capillary pressure increases as water saturation decreases as shown experimentally by Colbeck (1973). Thus at high water saturations where P_c is small, the surface temperature is high and heat flow into the interparticle contact causes rapid densification. As water saturation is reduced and capillary pressure increases, the rate of densificaton is reduced accordingly. The experimental results of Tusima (1973) and Kinosita (1963) demonstrate this fact. In principle the capillary pressure effect could be as large as -0.01 °C and have a profound effect on the response of wet snow to stress. In practice, however, this effect is greatly reduced by the time required to achieve large capillary pressures in large-grained materials. Harris and Morrow (1964) showed that reduction of liquid pressure is delayed during drainage because of the slow process of liquid movement through thin films on particle surfaces. Harris and Morrow's results suggest that Colbeck's (1973) capillary pressure - water saturation curve does not quite represent true capillary equilibrium because the experiment was completed too quickly to allow complete drainage at each pressure level. Thus while capillary pressure can have a large effect on the densification of wet snow, there may be a time lag of days required for complete liquid drainage from wet snow subjected to large capillary pressures. Much experimental work remains to be done on the capillary equilibrium in the pendular regime of saturation to determine under what circumstances it is possible to achieve large capillary pressures in wet snow samples. The main problem is the loss of liquid contact between the sample and the porous plate through which the liquid is extracted. Occasionally it is possible to measure large capillary pressures in wet snow (Colbeck, 1976) suggesting that loss of contact cannot necessarily be predicted in advance. This problem, which is common for large grained, porous materials, does not preclude the application of this theory of thermodynamic densification to samples subjected to large capillary pressures. However, it must be recognized that large capillary pressures are difficult to obtain experimentally.

Heat and Mass Flow

When a lower temperature occurs at the inter-particle contact than at the particle surface, heat (Q) flows toward the contact at approximately

$$Q = k \frac{T_s - T_b}{r_b} \tag{4}$$

and the contact melts at a rate given by

$$\frac{dD}{dt} = \frac{k}{L\rho_s} \frac{T_s - T_b}{r_b} \tag{5}$$

where D is the total displacement of the contact (see Figure 2). Equation (5) gives the rate of approach of particle centers but the particle size, impurity level, water content and contact radius must be known to use this result. It is unlikely that the contact radius can be determined directly at any time for any given sample although most of the other parameters could be measured. Accordingly, it is necessary to either know the complete history of a sample of wet snow or to relate the contact size to density through assumptions about the geometry of particle arrangements. The latter is done in the next section.

Assuming a constant thickness for the water film at the contact, heat and water flow must balance. At normal rates of densification, the thickness of the water film at the contact is apparently many times thicker than an adsorbed layer of structured water hence the flux of water through the film is described by

$$q = \frac{d^3}{12\mu} \frac{\partial p}{\partial r} \qquad (6)$$

By continuity the flux of water increases with radius (r) along the contact as

$$q = \frac{\rho_s}{\rho_\ell} \frac{dD}{dt} \frac{r}{d} \qquad (7)$$

hence, for flat contacts, the pressure distribution along the water film,

$$p = p_o - \frac{6\mu}{d^4} \frac{\rho_s}{\rho_\ell} \frac{dD}{dt} r^2 \qquad (8)$$

is very sensitive to the thickness (d) of the film. For small increases in the size of the film, a large change in pressure and flux occurs, therefore, the film size is relatively stable for large fluctuations in heat and water flow. Unfortunately q and d cannot be identified independently without making some assumption about the pressure field. While this is not necessary here, it is important that pressure is not uniform along the contact. The pressure drop toward the outside of the contact is necessary to cause water flow out of the contact and into the pore space. The parabolic distribution given by Equation (8) shows a fairly uniform liquid pressure over most of the contact with a rapid pressure drop near the edge of the contact. Thus the water film is capable of supporting the force between the particles with a maximum pressure (p_o) only slightly higher than the average contact stress ($F\pi^{-1} r_b^{-2}$). It is now apparent that the liquid pore pressure affects both the phase equilibrium temperature of the pore space and the liquid pressure distribution in the contact. The first effect is manifested by a change in temperature distribution and rate of densification while the second effect influences only the thickness of the liquid layer at the contact.

Particle Geometry

The rate at which the particle centers move closer together by contact melting can be calculated with Equation (5) but it is necessary to specify the packing geometry to construct a model of wet snow densification. Visscher and

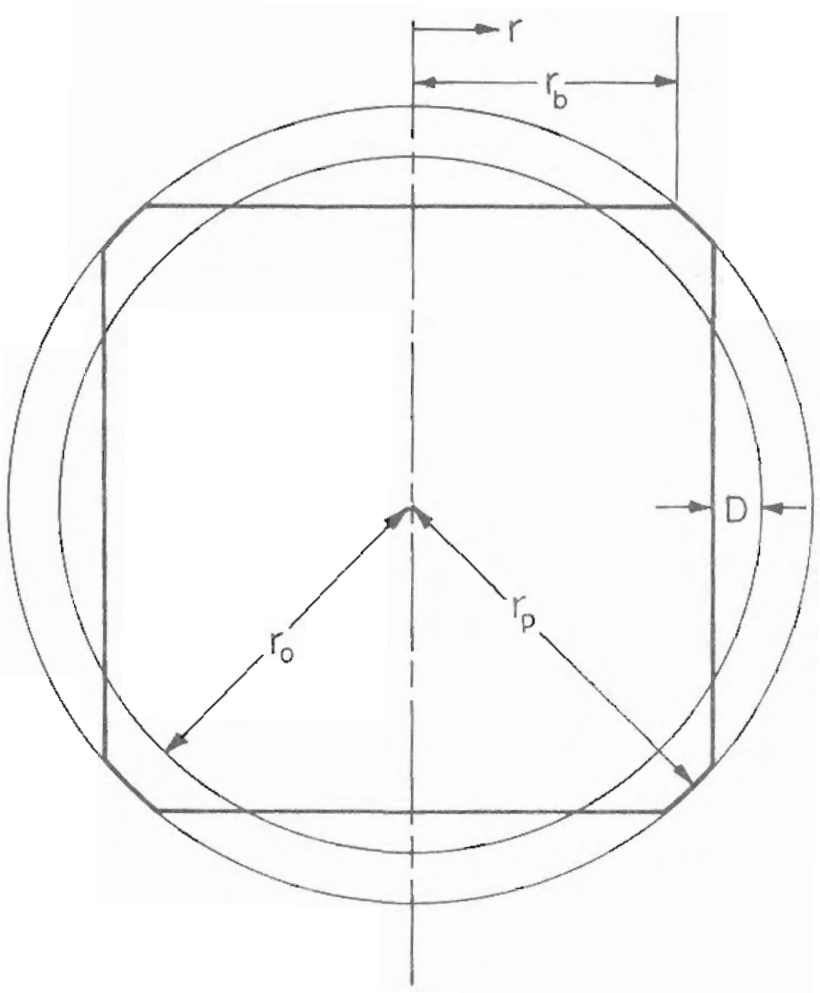

Figure 2.

A cross-sectional view through the center of a sphere showing the initial radius (r_o), contact displacement (D), contact radius (r_b), and current particle radius (r_p).

Bolsterli (1972) found an average of 6.4 contacts per sphere in random packings of uniform spheres. This is closely approximated by the geometrically regular, cubic packing which considerably simplifies the complicated geometry of a random packing. The disadvantage of using a cubic model is describing densification at porosities greater than 0.476. Higher porosities may be represented by allowing the number of contacts to increase to six as the 0.476 porosity is approached, however, some experimental testing of this approach must be made prior to its adoption.

Starting with a cubic packing of equal spheres, densification proceeds by melting at interparticle contacts and refreezing in the pore space. The mass of each particle is constant and we assume, except for its six contact surfaces, each particle remains spherical. At any time during densification the displacement (D) is (see Figure 2)

$$D = r_o - (r_p^2 - r_b^2)^{1/2} \tag{9}$$

and the ice density of the sample is

$$\rho = \rho_o \left(\frac{r_o}{r_o - D}\right)^3 \tag{10}$$

The intersecting volumes of the contact surfaces add some error to these equations at higher densities but this error is less than one percent. The particle radius increase associated with the refreezing in the pore space is 14 percent of the initial radius for the cubic model and must be accounted for in the model.

Since mass is conserved for each particle, the particle radius (r_p) and contact radius (r_b) are related to the initial radius (r_o) by

$$r_o^3 = 4r_p^3 - 3(r_p^2 - r_b^2)^{3/2} - 4.5\, r_b^2\, (r_p^2 - r_b^2)^{1/2} \tag{11}$$

In principle it is now possible to solve for $\rho(t)$ for any given set of conditions but the algebraic barrier makes this approach impractical and an iterative calculation of the deformation starting from the cubic packing of equal spheres is used instead. As an example of the geometrical relationships and as an aid in the iterative calculation, D and r_b are shown as functions of r_p on Figure 3.

Results of the Model

As an example of the application of these concepts, the hydrostatic compression of saturated snow at a hydrostatic stress of 10^4 N/m^2 is calculated. Calculated values at steps in the iterative procedure are given in Table 1 and the results are shown on Figure 4. The size of the melt cap (D) increases rapidly at first because of the high stress concentration at the points of the spherical particles but the rate of growth of the cap decreases as the cap area increases. Likewise, the rate of density increase is a steadily decreasing function of time and approaches the density of solid ice assymtopically. Qualitatively these results are very similar to those of Tusima (1973) although his tests were done with repeated loadings at a stress of 3.25×10^5 Nm^{-2} and

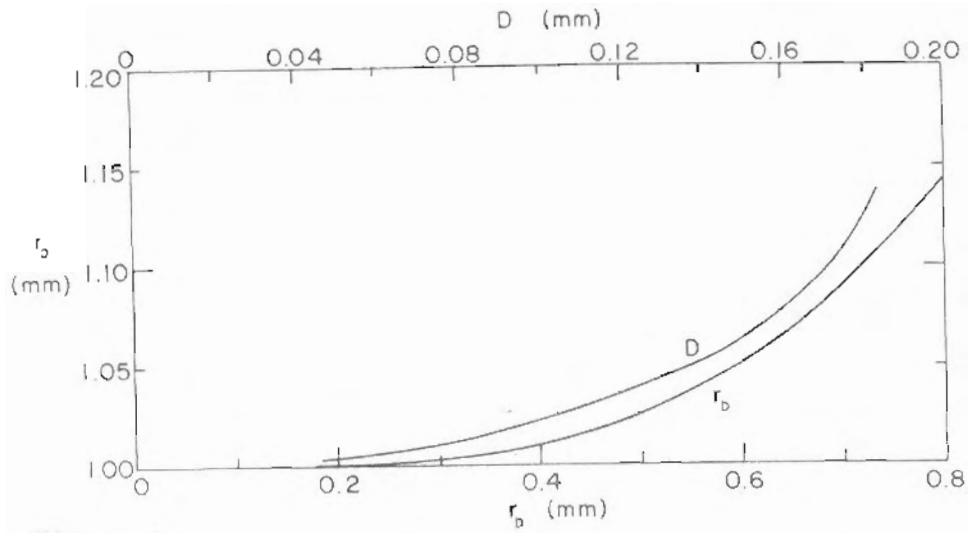

Figure 3.

The contact displacement (D) and bond radius (r_b) are shown as of function of particle radius (r_p) for a particle of initial radius (r_o) of 1 mm.

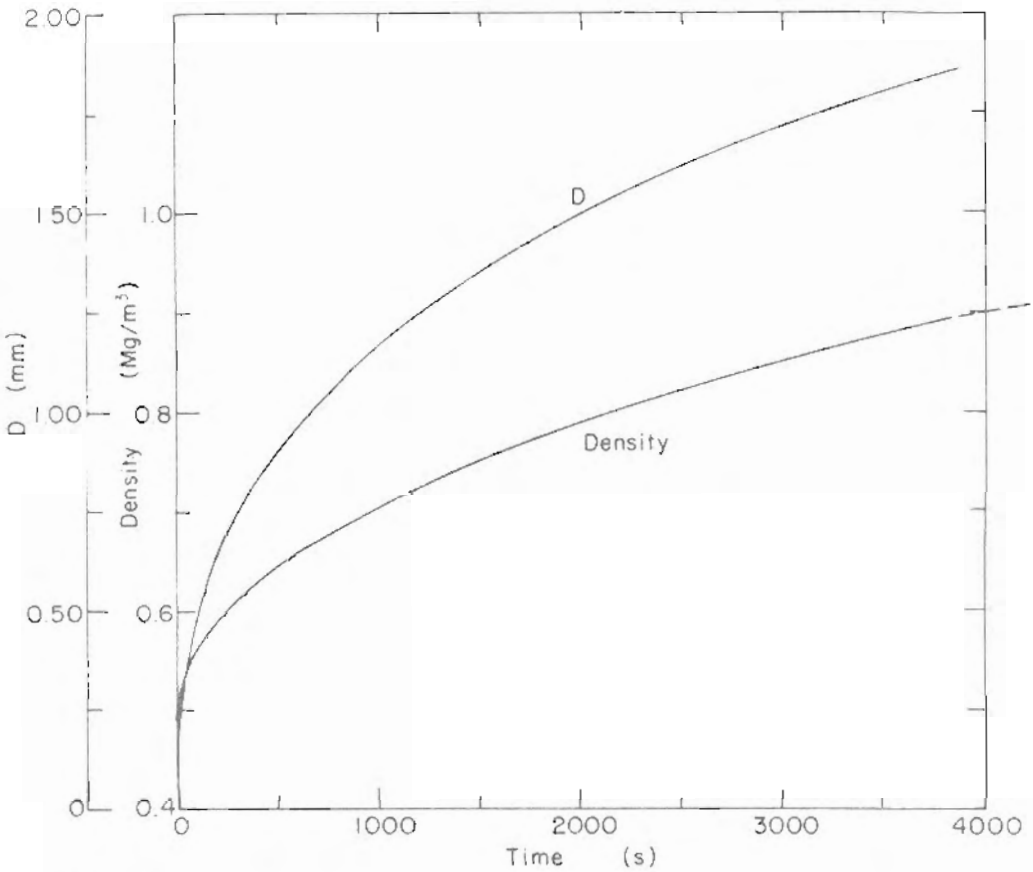

Figure 4.

The ice density and size of the melted cap (D) are shown as functions of time for a saturated sample compressed hydrostatically with a stress of 10^4 N/m^2.

Table I. The hydrostatic compression of saturated snow at 10^4 N m^{-2}.

r_p (mm)	r_p (mm)	D (mm)	dD/dt (mm s^{-1})	ρ (kg m^{-3})	P_b (N m^{-2})
1.0	0.	0	0	480	0
1.003	0.295	0.0413	$2{,}078 \times 10^{-7}$	445	112,000
1.01	0.4	0.072	$1{,}060 \times 10^{-7}$	602	68,100
1.022	0.487	0.101	618×10^{-7}	662	44,800
1.038	0.589	0.125	383×10^{-7}	718	31,100
1.062	0.634	0.149	262×10^{-7}	780	22,800
1.105	0.731	0.172	168×10^{-7}	845	16,050

The rate of density increase is a complicated function of stress because of the complicated relationships among the thermodynamic and geometrical variables which control the rate of density increase. However, as shown on Table 2, the rate of growth of the melt cap increases approximately linearly with the increase in stress. Therefore the rate of increase in density,

$$d\rho/dt = \frac{3\,\rho_o r_o^3}{(r_o - D)^4}\, dD/dt \qquad (12)$$

is approximately linearly related to stress when the load is first applied, but is a nonlinear function of stress at larger values of time because the denominator of Equation (12) decreases with increasing deformation.

The decrease in phase equilibrium temperature associated with increasing capillary pressure decreases the heat flow from the particle surface to the inter-particle bond as described previously. Thus at lower liquid saturations, the thermodynamic deformation of wet snow proceeds more slowly as shown by Tusima's (1973) results on Figure 5. Tusima's data suggest that the maximum density approaches a lower limit at lower water saturations, an expected result of lowering the phase equilibrium temperature on the particle's curved surface. As a further example of the effect of capillary pressure on the rate of deformation of wet snow, the calculated densities are shown as functions of time at a hydrostatic stress of 10^4 N/m^2 and capillary pressures of 0, 0.1, 0.5 and 1 m of water (0, 987, 4935 and 9370 N/m^2) on Figure 6 and Table 3. Although the stress levels were higher in Tusima's experiments and the stress was applied intermittently, Tusima's results shown on Figure 5 are very similar qualitatively to the theoretical results shown on Figure 6. The rate of density increase is a decreasing function of time and, at lower water saturations corresponding to larger capillary pressures, the maximum density approaches a lower limit asymptotically. Once this limit is reached, further compression is only possible by more efficient particle packings or intracrystalline deformation. The former is not an effective mechanism at these higher densities while the latter occurs much more slowly than the thermodynamic metamorphism described here.

The presence of ionic impurities in the liquid phase has a dramatic effect on the mechanical properties of wet snow because the phase equilibrium temperature of the mixture is reduced. When sufficient impurities are present, the mixture temperature can be lowered beneath the inter-particle bond temperature in which case the bonds freeze and a significant inter-particle strength develops. Even if the bonds do not freeze, the heat flow away from the bonds is reduced and the rate of densification and the maximum density are reduced accordingly. Thus ionic impurities in dilute concentrations have the same effect on mechanical properties as capillary pressure. To illustrate this effect, the calculated curves on Figure 6 could be described as the effects of 0, 4.32×10^{-4}, 2.18×10^{-3} and 4.36×10^{-3} g-moles of sodium chloride per Kg of water in saturated snow instead of capillary pressures of 0, 987, 4935 and 9870 N/m^2 respectively. Since these levels of ionic impurities are not generally found in natural snowcovers away from contaminants such as road salt, it is concluded that capillary pressure is generally a more important parameter than concentrations of ionic impurities. The effect of impurities is clearly demonstrated and their use for strengthening snow surfaces as an aid in oversnow mobility is obvious. Like

Table II. The hydrostatic compression of saturated snow at two stresses.

(mm)	dD/dt (10^4 N m^{-2}) (mm s^{-1})	dD/dt (10^6 N m^{-2}) (mm s^{-1})
1.0	∞	∞
1.003	$2{,}078 \times 10^{-7}$	$2{,}100 \times 10^{-5}$
1.01	$1{,}060 \times 10^{-7}$	$1{,}070 \times 10^{-5}$
1.022	618×10^{-7}	622×10^{-5}
1.038	383×10^{-7}	391×10^{-5}
1.062	262×10^{-7}	268×10^{-5}
1.105	168×10^{-7}	173×10^{-5}

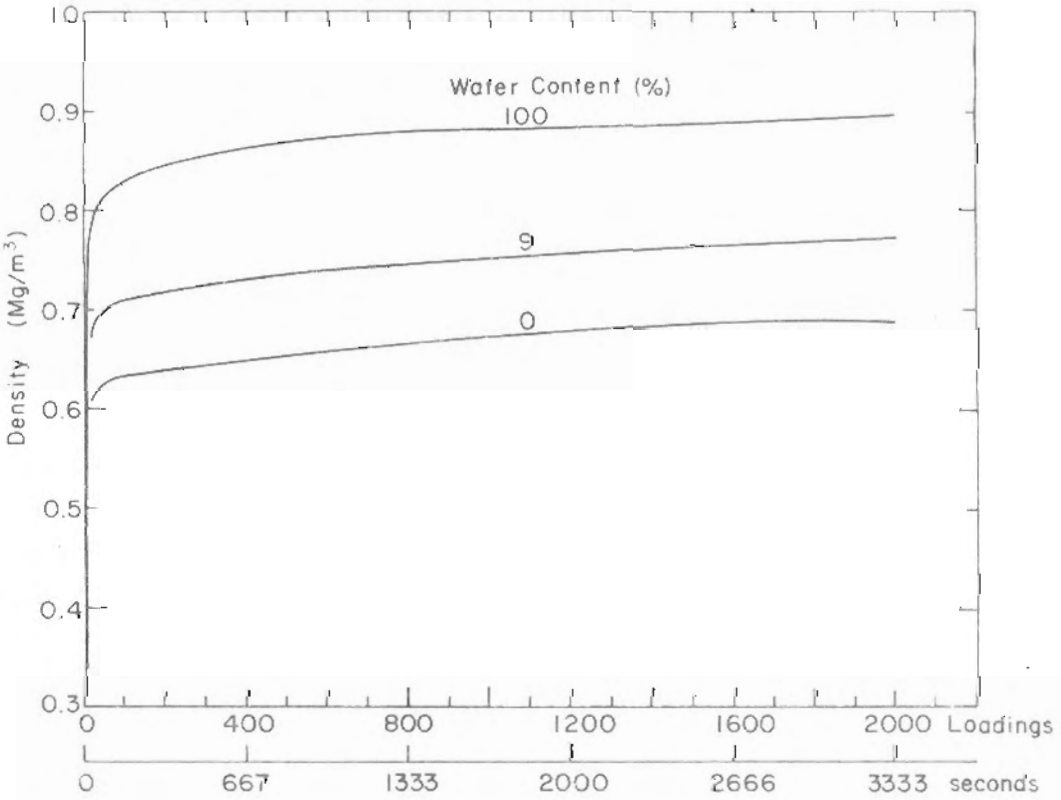

Figure 5.

Density is shown as a function of time for tests at three water saturations. The samples were repeatedly loaded (36 loads per minute) with a stress of 3.25×10^5 N/m^2. These curves were drawn from data taken from Tusima (1973).

Table III. The calculated deformation rates are shown for a hydrostatic stress of 10^4 N m^{-2} for four values of capillary pressure.

r_p (mm)	r_b (mm)	D (mm)	ρ (Mg m^{-3})	P_c=0 $d\rho/dt$ (Mg m^{-3} s^{-1})	0.1 $d\rho/dt$ (Mg m^{-3} s^{-1})	0.5 $d\rho/dt$ (Mg m^{-3} s^{-1})	1.0 m H_2O $d\rho/dt$ (Mg m^{-3} s^{-1})
1	0	0	0.480	∞	∞	∞	∞
1+	0.164	0.136	0.5046	0.00237	0.00231	0.00210	-
1.001	0.221	0.0236	0.516	9.64×10^{-4}	9.14×10^{-4}	7.46×10^{-4}	5.36×10^{-4}
1.002	0.265	0.0338	0.532	5.64×10^{-4}	5.21×10^{-4}	3.75×10^{-4}	1.93×10^{-4}
1.005	0.336	0.0527	0.565	2.89×10^{-4}	2.53×10^{-4}	1.28×10^{-4}	-
1.01	0.400	0.0724	0.602	1.78×10^{-4}	1.45×10^{-4}	3.08×10^{-4}	-
1.02	0.475	0.0975	0.653	1.11×10^{-4}	8.00×10^{-5}	-	-
1.04	0.566	0.128	0.724	6.98×10^{-5}	3.99×10^{-5}	-	-
1.05	0.600	0.138	0.750	5.99×10^{-5}	3.03×10^{-5}	-	-
1.075	0.677	0.157	0.802	4.52×10^{-5}	1.62×10^{-5}	-	-
1.10	0.722	0.170	0.839	3.66×10^{-5}	8.19×10^{-5}	-	-
1.14	0.794	0.182	0.877	2.80×10^{-5}	7.96×10^{-5}	-	-
1.146	0.804	0.183	0.881	2.71×10^{-5}	2.24×10^{-5}	-	-

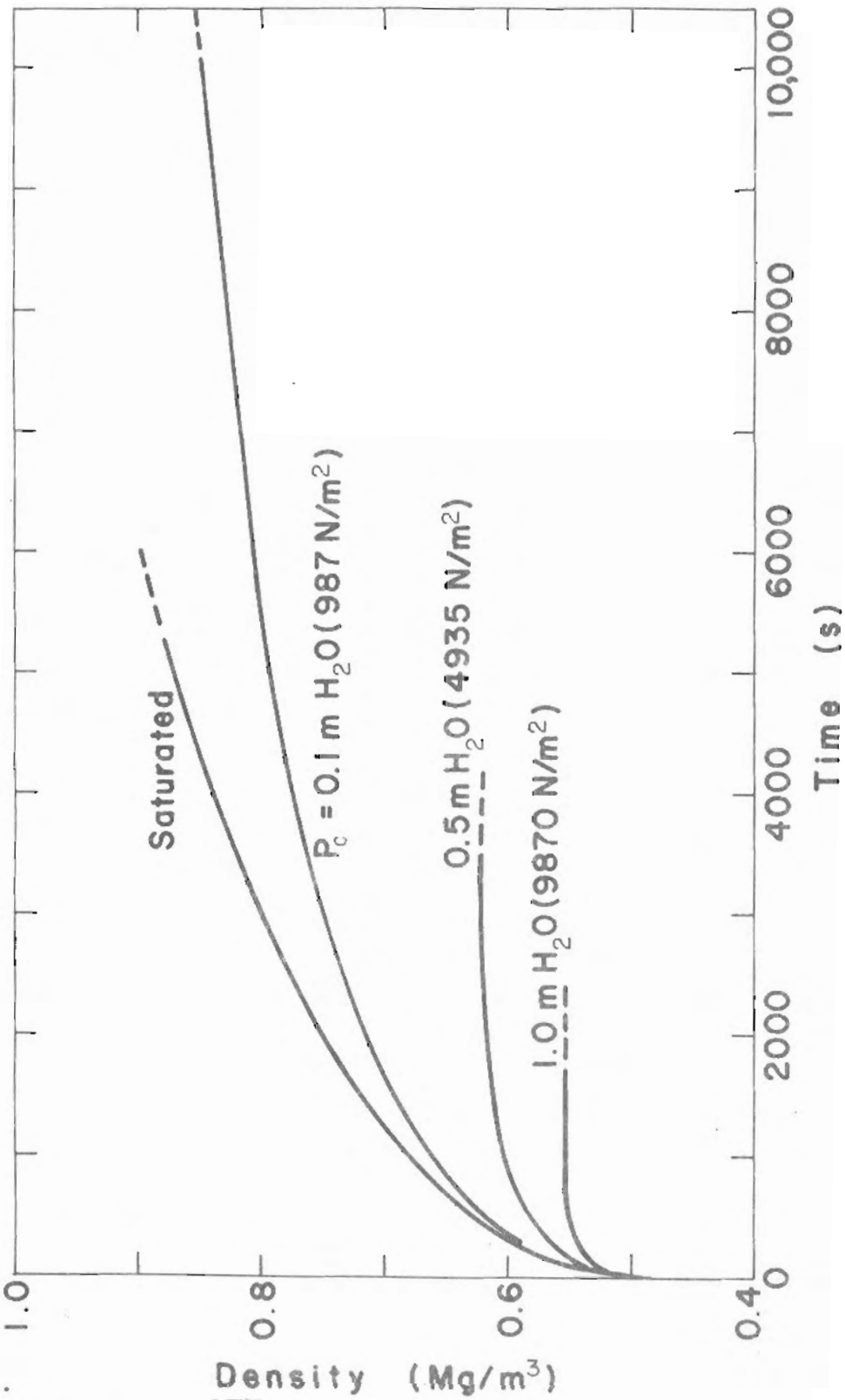

Figure 6.

The calculated density is shown as a function of time for four valves of capillary pressure at a hydrostatic stress of 10^4 N/m^2 and an initial particle size of 1 mm. At capillary pressures of 0.5 and 1 m H_2O, the maximum valve of density is reached. These four values of capillary pressure have the same effect as would sodium chloride concentrations of 0, 4.32×10^{-4}, 2.13×10^{-3} and 4.36×10^{-3} g-moles per Kg of water in saturated snow at the same stress.

capillary pressure, ionic impurities limit the thermodynamic densification of wet snow by lowering the phase equilibrium temperature at the curved particle surface. For any given stress and initial particle size, the inter-particle bonds develop to a certain size before thermal equilibrium is reached. The limiting inter-particle bond radius, r_b, is shown on Figure 7 as a function of sodium chloride concentration. The rapid thermodynamic densification of wet snow is limited according to the maximum size of the bond at equilibrium.

Nonhydrostatic Stress

The thermodynamic deformation of wet snow is most easily described when a hydrostatic, bulk stress causes isotropic densification. In that case all of the contacts in the cubic model experience equal stresses, temperatures and rates of melting. Other states of stress are more difficult to interpret but some important conclusions can be drawn. For example with confined compression, the lateral stresses are reduced by the viscous analogue of Poisson's ratio and, while the largest deformation will occur along the axis of compression, the lateral stresses will give some lateral deformation. In a model where a constant sample area is maintained, a rearrangement of the particles must occur to maintain a constant cross-sectional area. The cubic model can only account for this rearrangement by allowing the discreet motion of particles to ensure a complete packing of particles in the sample area. Thus the deformation along the axis of compression would be the sum of contact melting along that axis plus particle displacement to account for contact melting in the lateral direction. Other states of stress can be treated by similar techniques.

If one of the principal stresses is tensial, the response of wet snow can be anywhere between immediate failure at melting bonds to considerable strength at frozen bonds. As described in the introduction, the difference between melting and frozen bonds is determined by parameters such as impurity content, water saturation, contact size and history of the sample. If the bond survives the initial tensial loading, the equilibrium temperature would be raised by the tensial stress at the contact and freezing would strengthen the contact.

Conclusions

The thermodynamics of wet snow controls its rapid deformation in a manner unlike the deformation of dry snow. Because of the presence of liquid water, wet snow can deform rapidly by melting at the inter-particle contacts and refreezing at the curved ice surfaces. The rate of deformation is controlled by the paramenters which determine the temperature difference between the inter-particle contacts is determined strictly by the force between the particles and the size of the contact. The temperature of the curved surface is determined by the particle size, ionic impurity content of the liquid phase, and air bubble size or capillary pressure (depending on the saturation regime). As the inter-particle bond size increases, the inter-particle stress decreases and the bond temperature increases until the temperature differences around a particle are equalized. At that time rapid thermodynamic deformation ceases, and further deformation must proceed by more efficient packing arrangements and/or the normal processes of crystalline deformation.

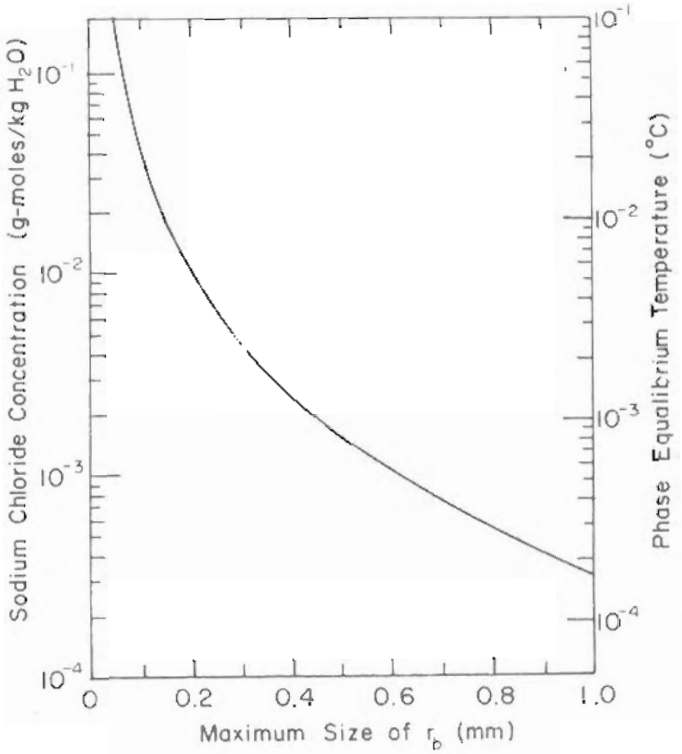

Figure 7.

The maximum radius of the inter-particle bond as a function of sodium chloride concentration is shown for an initial particle size of 1 mm and a bulk stress of 2320 N/m^2 in saturated snow. The bond size stops increasing when the pressure melting temperature of the bond surface equals the impurity temperature depression of the curved particle surface.

Using a simple geometric packing arrangement and the principles of thermodynamics, a simple model of wet snow deformation has been constructed. The results of this model are qualitatively similar to the experimental results of Tusima (1973), including a lower value of maximum density at larger capillary pressures. The effect of ionic impurities on the maximum bond size has also been calculated and found to be the same as increasing the capillary pressure. The hardening effects of increasing capillary pressure and/or ionic impurity content have practical implications for strengthening snow surfaces as an aid to oversnow mobility.

References

Colbeck, S.C. 1973. Theory of metamorphism of wet snow. U.S. Army Cold Regions Research and Engineering Laboratory Research Report 313.

Colbeck, S.C. 1976. On the use of tensiometers in snow hydrology. Journal of Glaciology, Vol. 17, No. 75, p. 135-40.

Harris, C.C. and N.R. Morrow. 1964. Pendular moisture in packings of equal spheres. Nature. Vol. 203, No. 4946, p. 706-08.

Kinosita, S. 1963. Compression of snow immersed in water of 0°C. I. Low Temperature Science, Series A, Vol. 21, p. 13-22.

Mellor, M. 1975. A review of basic snow mechanics. Snow Mechanics Symposium (Proceedings of Grindelwald Symposium, April 1974): IAHS Publ. No. 114, p. 251-91.

Moore, P.J. and D.V. Millar. 1971. The collapse of sands upon saturation. In Proceedings of the 1st Australian-New Zealand Conference on Geo mechanics, Vol. 1, p. 54-60.

Skelton, J. 1975. Interfibre forces during wetting and drying. Science, Vol. 190, No. 4209, p. 15-20.

Tusima, K. 1973. Tests of the repeated loadings on snow. Low Tem perature Science, Series A, Vol. 31, p. 57-68.

Visscher, W.M. and M. Bolsterli. 1972. Random packing of equal and unequal spheres in two and three dimensions. Nature. Vol. 239, p. 504-07.

Wakahama, G. 1968. The metamorphism of wet snow. In IUGG General Assembly of Bern, Sept.-Oct. 1967, p. 370-79.